

Exploiting Natural Dynamics in the Control of a 3D Bipedal Walking Simulation

Jerry E. Pratt and Gill A. Pratt

MIT Leg Laboratory

www.ai.mit.edu/projects/leglab

Abstract

Natural dynamics can be exploited in the control of bipedal walking robots: the swing leg can swing passively; a kneecap can prevent the leg from inverting; and a compliant ankle can naturally transfer the center of pressure along the foot and help in toe off. These mechanisms simplify control and result in motion that is smooth and natural looking.

We describe a computationally efficient algorithm which exploits these natural mechanisms. This algorithm is an extension to one for planar walking [16]. Lateral stability is controlled via foot placement and ankle torque.

We present results for a seven link, twelve degree of freedom, biped simulation which walks on flat ground.

1 Introduction

Many researchers [1, 4, 5, 6, 11], starting with McGeer and his passive dynamic walker, have exploited natural dynamics in order to make walking machines which are fully passive. These devices rely completely on their dynamics, and interaction with gravity, in order to walk.

Passive walkers have limitations, of course, such as limited capabilities and the need to walk down a slope. Powered robots [7, 18, 17, 15, 3, 9, 10, 12, 21, 22] can avoid these limitations. However, the control of powered bipedal robots has often been very complicated and the resultant motion often looks unnatural and is inefficient. Many of the controllers for powered robots are model based, requiring an accurate model of the dynamics of the robot in order to work. Several of the robots use trajectory tracking approaches which require pre-specified trajectories of either the body or the joints themselves.

In this paper, we describe an approach to powered bipedal walking which exploits the natural dynamics of the robot and requires only a simple control algorithm. We exploit three different natural mechanisms. We use a knee cap to prevent the leg from inverting, which makes height control easy. We use a compliant ankle limit so that the center of pressure on the foot travels forward with the center of mass of the body. And we exploit the natural swing dynamics of the leg to make swing control simple and natural looking.

We present an algorithm, following this approach, for the control of a three dimensional bipedal walking simulation. The algorithm is a direct extension of the algorithm we presented in [16] for planar bipedal walkers, with lateral motion stabilized through

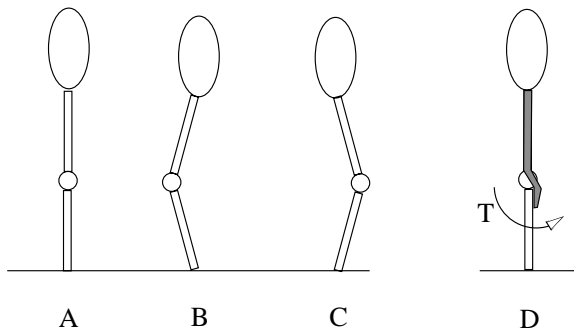


Figure 1: Diagram illustrating kneecap advantages. Without a kneecap, a biped with a straight support leg is in an unstable buckling configuration (A). Feedback control will result in chatter between knee inflections B and C due to delay, etc. With a kneecap (D), a constant torque with no feedback is enough to stabilize the system against buckling.

foot placement and ankle torque. The algorithm does not require dynamic modeling or inversion nor does it require reference trajectories. Video, data, source code, and more information can be found at <http://www.ai.mit.edu/projects/leglab/robots/m2/clawar99/>

2 Natural Dynamic Mechanisms

2.1 Knee Cap

Walking with straight support legs is more efficient than with bent legs since energy requirements in muscles and motors are proportional to the torque at the joint, even if there is no velocity. However, since the leg must support the weight of the body, a straight leg poses an interesting challenge. Figure 1 illustrates the issue. When the body is directly over the foot (A), no torque is required at the knee. However, this is an unstable latch configuration. If the knee moves slightly either way, the leg will buckle (B or C). It is challenging to control this situation. Due to controller non-idealities (bandwidth limitation, delays, etc.) a straight knee controller will typically exhibit chatter between configurations B and C.

Adding a knee cap (D) can greatly simplify the control and make the resultant motion smoother and more efficient. In fact, applying a constant torque so that the knee pushes against the stop will keep the leg straight. Of course other techniques can be used. Also, if the line of force on the body passes in front of the kneecap, the knee will be locked against the kneecap without any actuator torque.

Note that a rigid kneecap can be simulated if a small integration time step is used and no delays or filtering takes place. On a real robot with bandwidth limited actuators however, a physical kneecap is required to prevent chatter.

2.2 Compliant Ankle

Feet and ankles provide many benefits to bipedal walking. They reduce velocity fluctuations since the center of pressure on the foot can travel forward, staying below the center of mass of the body through part of the stride. They also help to control speed and to inject energy at the end of the stride through toe off.

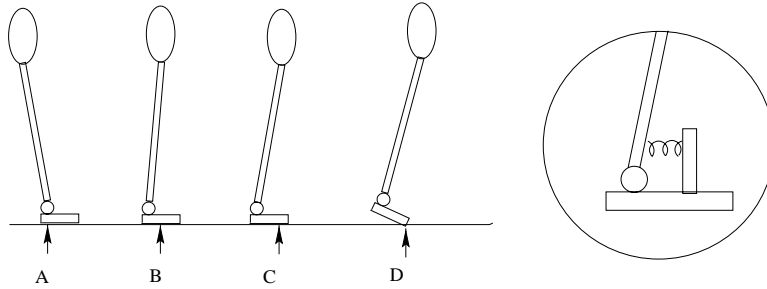


Figure 2: Diagram illustrating compliant ankle. In normal walking, the center of pressure on the foot travels forward as the center of mass travels forward (A-D). A compliant ankle (insert) can naturally achieve this effect. However, energy injection at toe off requires actuation.

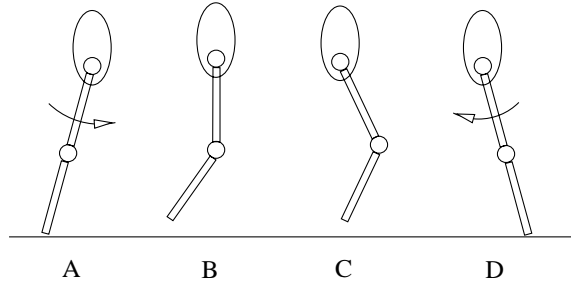


Figure 3: Diagram illustrating passive swing. Swing is initiated (A) through a forward torque on the hip, supplied either by hip actuators or gravity. The leg can swing passively (B - C) until swing is stopped (D) through a backward torque on the hip, again supplied either by hip actuators or gravity.

The torque at the ankle can be controlled actively. However, torque requirements can be quite high, since the foot provides a significant lever arm when the center of pressure is near the toe. A compliant ankle provides most of the benefits of a foot and ankle but without the actuator torque requirements. An actuator can then be used in addition to the passive ankle for fine control and energy injection at toe off. Figure 2 illustrates the situation. In configuration A, the center of mass is behind the foot and there is zero ankle torque. In configurations B and C, the center of mass is traveling forward. The passive ankle torque increases, thereby moving the center of pressure of the foot forward from the heel to the toe. In configuration D, the robot goes into toe off, releasing the energy stored in configurations B and C and perhaps injecting some more, through active torques, to maintain walking. The inset shows a simple spring configuration which can give the ankle the desired compliance.

Choosing an adequate spring torque versus displacement curve is important in achieving the desired behavior. For the simulation discussed below we use a quadratic spring ($\tau = k(\theta - \theta_0)^2$) and tune the stiffness parameter.

2.3 Passive Swing Leg

Most powered bipedal walkers use control techniques similar to those used for robotic arms to control the swing leg along a trajectory to a desired landing position. However, with a suitable leg, the natural swing dynamics are such that once the swing starts, the leg will

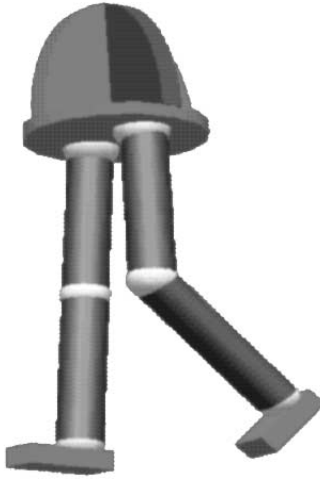


Figure 4: Three Dimensional bipedal walking simulation. The robot has twelve degrees of freedom: three in each hip, one in each knee, and two in each ankle.

Table 1: Physical parameters of the simulated bipedal walker. The center of mass of all links are located at their centroid. The first length is the distance of the body center of mass above the hip. The second length is the separation distance between the hips. The moments of inertia are calculated about the center of mass of each link.

Length (m)	hip to body	hip sep.	thigh	shin	foot length	width	height		
	.160	.184	.432	.432	.203	.089	.051		
Mass (kg)	body		thigh		shin		foot		
	12.75		2.74		2.70		0.66		
Inertia (kgm^2)	body Ixx,yy	Izz	thigh Ixx,yy	Izz	shin Ixx,yy	Izz	foot Ixx	Iyy	Izz
	.23	.21	.044	.004	.054	.003	.001	.002	.002

continue without any intervention, as illustrated in Figure 3. Gravity alone can be used to initiate swing, as in the case of the passive dynamic walkers. Hip torque can be added in order to make the leg swing faster, which is required for fast walking.

We use the passive swing properties of the leg in the control of our simulation. The hip is servoed forward to a desired angle and the knee is allowed to swing freely, with a little damping. At the end of the swing the knee is locked once it hits the knee cap.

In the next section, we describe an algorithm which exploits the three natural mechanisms, described above, in the control of a simulated bipedal robot.

3 Simulation Algorithm

We use the natural dynamic mechanisms described above in the control of a simulated seven link, twelve degree of freedom, bipedal robot. The rigid body simulation (Figure 4) is implemented using the Creature Library, an in-house software package based on SD-Fast of Symbolic Dynamics. The robot model has an actuated hip (3 dof), knee (1 dof), and ankle (2 dof) on each leg. The physical parameters (Table 1) were chosen to match those

of a bipedal robot currently under construction.

The simulation algorithm is summarized in Figure 5, with controller parameters in Table 2. Pitch, roll, and yaw are defined as if the body were an airplane: pitch corresponds to bending forward, roll to bending to the side, and yaw to twisting about the vertical axis. Each leg acts separately and has a simple state machine. The leg can be in either Support, Toe Off, Swing, or Straighten states.

In Support and Toe Off states, proportional-derivative (PD) controllers are used at the hip to servo body pitch, roll and yaw in order to maintain balance. Feed-forward torque is added to hip roll to offset the weight of the body:

```
tau.left_hip_pitch = -body_pitch_gain * (0.0 - q.pitch) + body_pitch_damp * qd.pitch;
tau.left_hip_roll = body_roll_gain * q.roll + body_roll_damp * qd.roll
                  + (HIP_OFFSET_Y * cos(q.roll) + BODY_CG_Z * sin(q.roll)) * ff_z;
tau.left_hip_yaw = body_yaw_gain * (q.yaw - q.d.yaw) + body_yaw_damp * qd.yaw;
```

where τ is the vector of joint torques, q is the vector of joint positions, and qd is the vector of joint velocities. Note that only the left leg is presented in all the code fragments.

In Support and Toe Off states, the knee is locked to maintain height:

```
tau.left_knee = knee_gain * (0.0 - q.left_knee) - knee_damp * qd.left_knee;
```

In Support state, the ankle pitch is unactuated - only the passive ankle compliance is present. The ankle roll is used to dampen lateral velocity, as described in Section 3.1. During Toe Off state, the ankle is servoed to an angle using a PD controller in addition to its passive compliance:

```
tau.left_ankle_pitch = push_gain * (push_set - q.left_ankle_pitch)
                    - push_damp * qd.left_ankle_pitch;
if (q.left_ankle_pitch < ankle_limit_set)
    tau.left_ankle_pitch = tau.left_ankle_pitch + ankle_limit_gain
                        * (ankle_limit_set - q.left_ankle_pitch)^2;
```

The transition from Support to Toe Off occurs when the heel lifts off the ground due to the passive compliance of the ankle.

The robot transitions from Toe Off to Swing when the force on the foot falls below a certain threshold. In both Swing and Straighten states the hip pitch is servoed to an angle using a PD controller:

```
Swing: tau.left_hip_pitch = hip_gain * ((-hip_d - q.pitch) - q.left_hip_pitch)
        - hip_damp * qd.left_hip_pitch;
Straighten: tau.left_hip_pitch = hip_gain * ((-hip_hold - q.pitch) - q.left_hip_pitch)
        - hip_damp * qd.left_hip_pitch;
```

The foot is servoed to be level with the ground so that the robot does not stub its toe. In Straighten state, the hip roll is used for lateral foot placement, to control lateral velocity, as described in Section 3.1. In Swing state, the knee is lightly damped while in Straighten state the knee is locked straight using a PD controller:

```
Swing: tau.left_knee = -swing_damp_knee * qd.left_knee;
Straighten: tau.left_knee = straighten_gain_knee * (0.0 - q.left_knee)
                - straighten_damp_knee * qd.left_knee;
```

The robot transitions from Swing to Straighten state after a constant amount of time passes. Finally, the robot transitions from Straighten to Support state when the heel of the swing leg hits the ground.

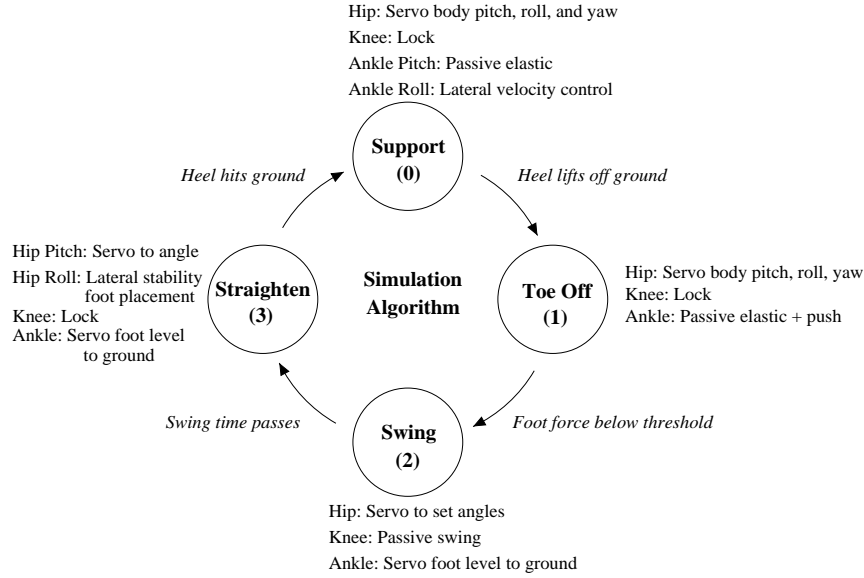


Figure 5: Simulation Algorithm. Each leg has a state machine which is in one of four states. State transition conditions and actions in each state are shown.

Table 2: Control system parameters of the simulated bipedal walker.

Controller Parameter	Value	Controller Parameter	Value
SUPPORT		SWING	
Body pitch gain	$100 \frac{Nm}{rad}$	Hip pitch set point	$0.625 rad$
Body pitch damping	$20 \frac{Nm}{rad/s}$	Hip pitch gain	$23.7 \frac{Nm}{rad}$
Body roll gain	$200 \frac{Nm}{rad}$	Hip pitch damping	$2.37 \frac{Nm}{rad/s}$
Body roll damping	$20 \frac{Nm}{rad/s}$	Max hip pitch torque	$10 Nm$
Body yaw gain	$30 \frac{Nm}{rad}$	Hip roll gain	$92 \frac{Nm}{rad}$
Body yaw damping	$4 \frac{Nm}{rad/s}$	Hip roll damping	$23 \frac{Nm}{rad/s}$
Knee gain	$30 \frac{Nm}{rad}$	Hip yaw gain	$9.2 \frac{Nm}{rad}$
Knee damping	$10 \frac{Nm}{rad/s}$	Hip yaw damping	$5.75 \frac{Nm}{rad/s}$
Passive ankle set point	$0.0 rad$	Knee damping	$0.25 \frac{Nm}{rad/s}$
Passive ankle spring constant	$400 \frac{Nm}{rad^2}$	Ankle gain	$4.0 \frac{Nm}{rad}$
Ankle lateral set point	$0.087 rad$	Ankle damping	$0.5 \frac{Nm}{rad/s}$
Ankle lateral speed gain	$0.36 \frac{rad}{m/s}$	Swing time	$0.3 sec$
Ankle roll gain	$100 \frac{Nm}{rad}$	STRAIGHTEN	
Ankle roll damping	$0.10 \frac{Nm}{rad/s}$	Hip pitch set point	$0.55 rad$
TOE OFF		Hip roll offset	$0.048 rad$
Ankle pitch set point	$0.3 rad$	Hip roll lateral speed gain	$0.36 \frac{rad}{m/s}$
Ankle pitch gain	$30 \frac{Nm}{rad}$	Hip roll lateral position gain	$2.0 \frac{rad}{m}$
Ankle pitch damping	$0 \frac{Nm}{rad/s}$	Knee gain	$1.0 \frac{Nm}{rad}$
Swing transition foot force	$100 N$	Knee damping	$1.2 \frac{Nm}{rad}$

3.1 Lateral Stability

To control lateral stability in the frontal plane, we use foot placement and ankle torque. Since our control algorithm treats the frontal plane dynamics and the sagittal plane dynamics separately, as though they were decoupled, we use a conservative approach for the frontal plane. On each step we attempt to place the foot such that lateral velocity will be absorbed into potential energy as the body moves directly over the support foot. In this way the body is “captured” laterally so that no matter what the forward velocity of the robot is, it will not start tipping back laterally until the body has traveled forward over the support foot.

Figure 6 shows a simple pendulum model for determining foot placement. The initial kinetic energy is

$$E_k = \frac{1}{2}mv^2 \quad (1)$$

The change in potential energy when the mass transfers from its initial condition to its highest point is

$$\Delta E_p = mgl(1 - \cos \theta) \quad (2)$$

Setting the change in potential energy equal to the kinetic energy we get

$$\cos \theta = 1 - \frac{v^2}{2gl} \quad (3)$$

For small angle approximation, we get

$$\theta = \frac{v}{\sqrt{gl}} \quad (4)$$

We use equation 4 for determining lateral foot placement. During the Straighten state, hip roll is servoed to a set point proportional to the robot’s lateral velocity (y_d) and proportional to the robot’s lateral position with respect to the support foot (r_{ceny}):

```
q_d.left_hip_roll = -q.roll + swing_roll_off;
q_d.left_hip_roll = q_d.left_hip_roll + yd_gain * yd + ceny_gain * r_ceny;
tau.left_hip_roll = hip_k * (q_d.left_hip_roll - q.left_hip_roll)
- hip_b * qd.left_hip_roll;
```

If the leg touches down at the proper angle, the mass will come to rest at the highest point, above the foot. However, there may be some error in the foot placement, and there will be errors due to the simplified model. To overcome these errors, we use ankle torque, after the foot is placed.

The ankle torque is limited due to the small width of the feet. A static analysis gives us,

$$-mgw_f \leq \tau_{ankroll} \leq mgw_f \quad (5)$$

where w_f is half the width of the foot. By examining the dynamics, one can show that the mass can be captured over the foot if,

$$\frac{v}{\sqrt{gl}} - \frac{w_f}{l} \leq \theta \leq \frac{v}{\sqrt{gl}} + \frac{w_f}{l} \quad (6)$$

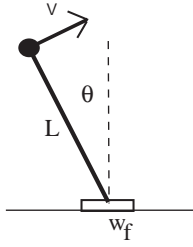


Figure 6: Simple pendulum model of the dynamics in the frontal plane. The robot mass is lumped at a point. This model is useful for studying the effects of foot placement and ankle torque on lateral velocity.

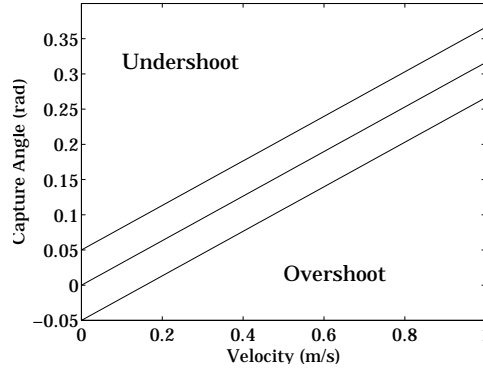


Figure 7: Range of Capture Angle vs. lateral velocity for a simple pendulum model with ankle torque. The middle curve is the leg angle required at foot placement in order for the mass to stop directly over the foot without using ankle torque. The outside curves show the range of leg angle which can result in capture with the use of ankle torque.

Equations 4 and 6 are plotted in Figure 7. The parameter values we use are $w_f = 0.05m$, $l = 1.0m$, $g = 10.0\frac{m}{s^2}$. The middle line is the touch down angle required to have the mass stop at rest above the foot (capture angle). The top and bottom lines show the range of angles at which the mass can be captured at the top with the aid of ankle torque. We see that ankle torque can compensate for errors in lateral foot placement, even with a narrow foot. In our simulation algorithm, we change the set point of the stance ankle roll based on the lateral velocity for capture, from Equation 4:

```
tau.left_ankle_roll = yd_ankle_gain
                    * ((-flat_ankle_roll - yd_gain * yd) - q.left_ankle_roll)
                    - ankle_b * qd.left_ankle_roll;
```

This can also be viewed as equivalent to a PD controller with constant set point and additional ankle torque proportional to lateral velocity.

3.2 Simulation Results

The simulation parameters were first manually tuned, and then fine tuned using a genetic algorithm with efficiency as its cost function. Efficiency was computed as distance traveled divided by total joint energy after ten seconds of walking. Total joint energy was computed by integrating the total joint power which is the sum of the absolute values of the mechanical power at each joint:

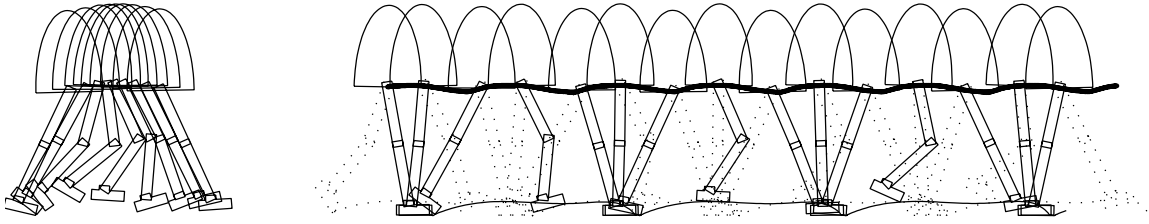


Figure 8: Elapsed time snapshot of the simulated robot walking data. The left leg is dotted while the right leg is solid. Lines show the path of the tips of the feet and the hip trajectory. The snapshots on the left are spaced at 0.1 seconds and show one swing phase. The snapshots on the right are spaced at 0.4 seconds and show several steps.

$$E_{tot} = \int P_{tot} dt, \quad P_{tot} = \sum_{joints} |P_{joint}|, \quad P_{joint} = \tau_{joint} \dot{\theta}_{joint} \quad (7)$$

After a couple generations, natural looking walking resulted. A time elapsed animation is shown in Figure 8. The drawings on the left show the swing phase of one leg. The drawings on the right show several steps. The right leg is dotted while the left leg is solid. Lines show the path of the tips of the feet and the hip trajectory. Results are plotted graphically in Figure 9.

We see that the simulated robot walked at a moderate speed (approximately 0.8 m/s) and had a natural looking gait. It is interesting that the algorithm does not contain any explicit speed control mechanism, yet speed is stabilized. We speculate that this is due to the natural system dynamics, in the same way that speed is naturally stabilized in the passive dynamic walkers.

4 Conclusions and Future Work

Three dimensional bipedal walking can be achieved by a simple control algorithm which exploits the natural dynamics of a kneecap, compliant ankle, and passive swing leg. Lateral foot placement and ankle torque can be used for lateral stability. The resultant motion is fairly smooth and efficient. This work may help bridge the gap between passive dynamic walkers and powered bipedal robots.

The simulation settles on a stable speed of walking of approximately 0.8 m/s. However, nowhere in the controller is speed explicitly controlled. We believe that the speed is stabilized in a similar way to passive dynamic walking machines. That is, if the robot goes too fast, it naturally takes a longer step due to the natural swing leg dynamics and hence slows down on the next step. Similarly, if the robot moves too slowly, it naturally takes a shorter step and hence speeds up on the next step. This behavior has also been observed in our experimental robot, Spring Flamingo.

In order to exploit the natural dynamics of a walking robot, it is important that the inertia and friction of the actuators does not dominate the dynamics of the legs. In our robots we use Series Elastic Actuators [14]. These actuators have good force dynamic range and low force offset which are important in natural and efficient walking. We are continuing to use these actuators in the design of several new walking robots.

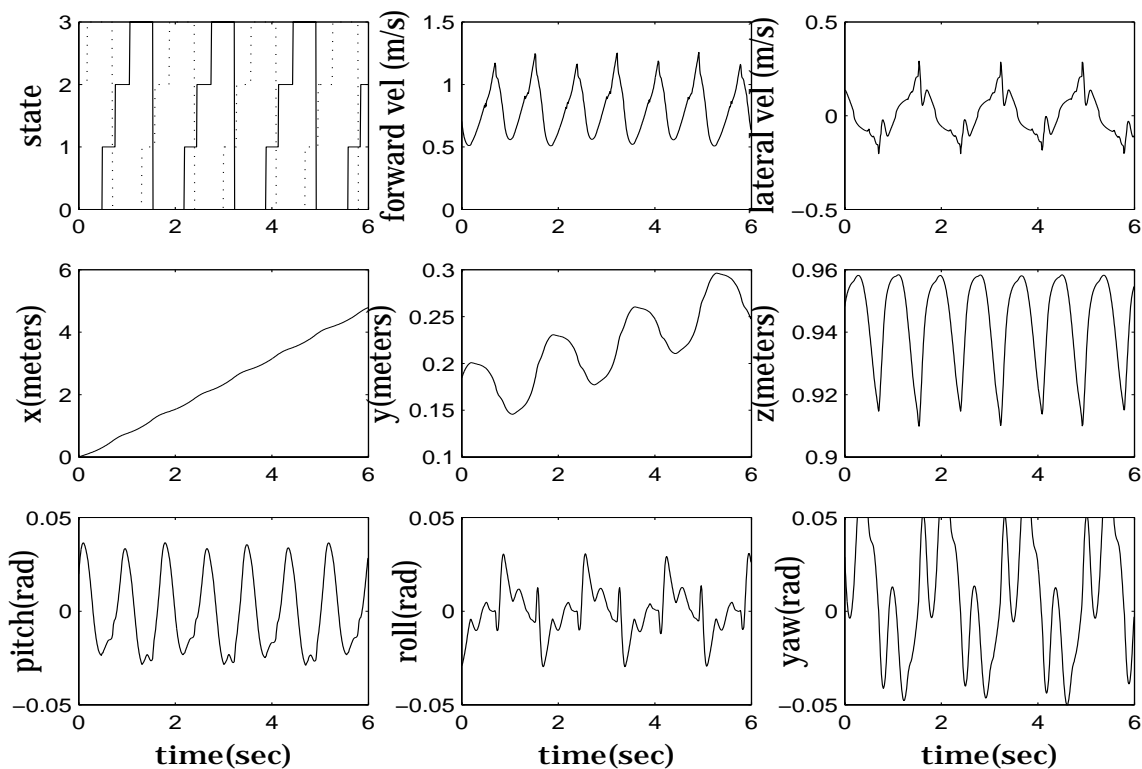


Figure 9: Simulation data. The first row contains, left to right, state of the legs, forward velocity, and lateral velocity. The second row contains forward distance, lateral motion, and body height. The last row contains body pitch, roll, and yaw.

The algorithm presented in this paper was for steady state walking. We are currently investigating transient conditions such as starting and stopping and dynamic turning.

References

- [1] J. Adolfsson, H. Dankowicz, and A. Nordmark. 3-d stable gait in passive bipedal mechanisms. *Proceedings of 357 Euromech*, 1998.
- [2] R. Q. Van der Linde. Active leg compliance for passive walking. *IEEE Conference on Robotics and Automation*, pages 2339–2345, 1998.
- [3] E. Dunn and R. Howe. Foot placement and velocity control in smooth bipedal walking. *IEEE Conference on Robotics and Automation*, pages 578–583, 1996.
- [4] J. Fowble and A. Kuo. Stability and control of passive locomotion in 3d. *Proceedings of the Conference on Biomechanics and Neural Control of Movement*, pages 28–29, 1996.
- [5] M. Garcia, A. Chatterjee, and A. Ruina. Speed, efficiency, and stability of small-slope 2d passive dynamic bipedal walking. *IEEE International Conference on Robotics and Automation*, pages 2351–2356, 1998.
- [6] A. Goswami, B. Espiau, and A. Keramane. Limit cycles in a passive compass gait biped and passivity-mimicking control laws. *Journal of Autonomous Robots*, 1997.
- [7] K. Hirai, M. Hirose, Y. Haikawa, and T. Takenaka. The development of honda humanoid robot. *IEEE Conference on Robotics and Automation*, 1998.

- [8] L. Jalics, H. Hemami, and B. Clymer. A control strategy for adaptive bipedal locomotion. *IEEE Conference on Robotics and Automation*, pages 563–569, 1996.
- [9] S. Kajita and K. Tani. Adaptive gait control of a biped robot based on realtime sensing of the ground profile. *IEEE Conference on Robotics and Automation*, pages 570–577, 1996.
- [10] A. Kun and W. T. Miller. Adaptive dynamic balance of a biped robot using neural networks. *IEEE Conference on Robotics and Automation*, pages 240–245, 1996.
- [11] Tad McGeer. Passive dynamic walking. *International Journal of Robotics Research*, 9(2):62–82, 1990.
- [12] H. Miura and I. Shimoyama. Dynamic walk of a biped. *International Journal of Robotics Research*, 3(2):60–74, 1984.
- [13] Simon Mochon and Thomas A. McMahon. Ballistic walking: An improved model. *Mathematical Biosciences*, 52:241–260, 1979.
- [14] Gill A. Pratt and Matthew M. Williamson. Series elastic actuators. *IEEE International Conference on Intelligent Robots and Systems*, 1:399–406, 1995.
- [15] J. Pratt, P. Dilworth, and G. Pratt. Virtual model control of a bipedal walking robot. *IEEE Conference on Robotics and Automation*, pages 193–198, 1997.
- [16] J. Pratt and G. Pratt. Exploiting natural dynamics in the control of a planar bipedal walking robot. *Proceedings of the Thirty-Sixth Annual Allerton Conference on Communication, Control, and Computing*, pages 739–748, 1998.
- [17] J. Pratt and G. Pratt. Intuitive control of a planar bipedal walking robot. *IEEE Conference on Robotics and Automation*, 1998.
- [18] Marc H. Raibert. *Legged Robots That Balance*. MIT Press, Cambridge, MA, 1986.
- [19] M. Vukobratovic, B. Borovac, D. Surla, and D. Stokic. *Biped Locomotion: Dynamics, Stability, Control, and Applications*. Springer-Verlag, Berlin, 1990.
- [20] Matthew M. Williamson. Exploiting natural dynamics in robot control. *Proceedings of the Fourth European Meeting on Cybernetics and Systems Research (EMCSR '98)*, 1998.
- [21] J. Yamaguchi, A. Takanishi, and I. Kato. Development of a biped walking robot adapting to a horizontally uneven surface. *IEEE International Conference on Intelligent Robots and Systems*, pages 1156–1163, 1994.
- [22] K. Yi and Y. Zheng. Biped locomotion by reduced ankle power. *IEEE Conference on Robotics and Automation*, pages 584–589, 1996.